Chapter 1

Decay and Amplification of Magnetic Fields

It's not whether a thing is hard to understand.
It's whether, once understood, it makes any sense.

Hans Zinsser
Rats, Lice and History (1934)

1.1 Preliminary considerations [Sprem]

1.1.1 The dynamo problem

The observations reviewed in the preceding chapter estalished rather unambiguously that the large-scale solar magnetic field is regenerated cyclically on a $\sim 22\,\mathrm{yr}$ timescale. In the MHD limit, the essence of this variation is embodied in the induction equation:

$$\frac{\partial \mathbf{B}}{\partial t} = \nabla \times (\mathbf{u} \times \mathbf{B}) - \nabla \times (\eta \nabla \times \mathbf{B}) \tag{1.1}$$

where the magnetic diffusivity η ($\equiv c/4\pi\sigma_e$) is inversely to the fluid's electrical conductivity σ_e. For physical conditions typical of the solar radiative interior, $\eta \sim 10^2$—$10^4\,\mathrm{cm}^2\,\mathrm{s}^{-1}$. It is worth pointing out that the solar interior is a much better electrical conductor than pure copper ($\eta \simeq 10^5\,\mathrm{cm}^2\,\mathrm{s}^{-1}$ at room temperature).

The diffusive term $-\nabla \times (\eta \nabla \times \mathbf{B})$ ($\equiv \eta \nabla^2 \mathbf{B}$ for constant η) on the RHS of the induction equation represents a sink of magnetic field; while diffusion can lead to the appearance of a field in regions previously devoid of it, in a global sense diffusion always destroys magnetic fields [1]. The induction term $\nabla \times (\mathbf{u} \times \mathbf{B})$ can, under certain conditions, act as a source of magnetic field. Note that there are no true source term in eq. (1.1); if $\mathbf{B} = 0$ at some t_0, then $\mathbf{B} = 0$ for all subsequent $t > t_0$.

Leaving cyclic variations aside for the moment, the crux of the dynamo problem is to establish the conditions under which a weak, pre-existing magnetic field can be amplified and maintained against Ohmic dissipation. In an electrically conducting fluid system such as the interior of the Sun, this will involve finding a smooth flow field $\mathbf{u}$ that has the adequate topological properties to lead to field amplification.

Now, you may recall from §I.1.1 that in general a Lorentz force

$$\mathbf{F}_L = \frac{1}{4\pi}(\nabla \times \mathbf{B}) \times \mathbf{B} \tag{1.2}$$

will be associated with the evolving magnetic field, and this Lorentz force can be expected to influence the driving fluid motions (cf. eq. [I.1.13]) for strong enough magnetic fields. The *kinematic regime* is that in which this backreaction on $\mathbf{u}$ is neglected, i.e., $\mathbf{u}$ is *specified a priori* and eq. (1.1) is solved independently of any equations of motion for $\mathbf{u}$. This drastic simplification carries the immense advantage that the induction equation is then linear in $\mathbf{B}$. In this and the following chapters we will concentrate mostly on this kinematic regime, but will occasionally flirt with the much more difficult dynamical problem.

It will often prove useful to work with the induction equation written in terms of a vector potential $\mathbf{A}$ such that $\mathbf{B} = \nabla \times \mathbf{A}$. Equation (1.1) is then readily be integrated to[2]:

$$\frac{\partial \mathbf{A}}{\partial t} = \mathbf{U} \times (\nabla \times \mathbf{A}) - \eta \nabla \times (\nabla \times A) \tag{1.3}$$

Clearly, any solution of eq. (1.3) identically satisfies the flux conservation constraint $\nabla \cdot \mathbf{B} = 0$. The first, almost trivial inference that can be drawn, from either eq. (1.1) or (1.3), is that a flow that is everywhere parallel to a magnetic field has no inductive effects.

[1] Can you think of a simple argument for why this is the case? If not go do problem (2.1) and return to this footnote.

[2] Strictly speaking, the "uncurling" of the original induction equation (1.1) generates an additional term on the RHS of eq. (1.3), having the form of the gradient of some scalar function. This term is set to zero here because it will play no role in anything to follow.

1.1.2 The magnetic energy

A useful (and important) quantitative measure of dynamo action, which will be encountered again and again below is the rate of growth of the magnetic energy $\mathcal{E}_B$ integrated over the entire spatial domain:

$$\mathcal{E}_{\rm B} = \frac{1}{8\pi} \int_V \mathbf{B}^2 {\rm d}V \tag{1.4}$$

In general, a flow will be deemed a dynamo if ${\rm d}\mathcal{E}_{\rm B}/{\rm d}t > 0$ for times much larger than all relevant advective and diffusive timescales of the problem.

An evolution equation for $\mathcal{E}_{\rm B}$ is readily obtained by dotting $\mathbf{B}$ into the original induction equation (1.1); after some vector algebraic manipulation and use of Gauss' theorem, one obtains

$$\frac{{\rm d}\mathcal{E}_{\rm B}}{{\rm d}t} = \tag{1.5}$$

1.1.3 The magnetic Reynolds number

The evolution of a magnetic field under the action of a prescribed flow $\mathbf{u}$ will depend greatly on whether or not the inductive term on the RHS of eq. (1.1) dominates the diffusive term. Under what conditions will this be the case? We seek a first (tentative) answer to this question be performing a dimensional analysis of eq. (1.1); this involves replacing spatial derivatives by $1/\ell$, where ℓ is a typical length over which $\mathbf{B}$ varies appreciably. This yields

$$\frac{\partial \mathbf{B}}{\partial t} = \frac{u_0 \mathbf{B}}{\ell} + \frac{\eta \mathbf{B}}{\ell^2} \tag{1.6}$$

where u_0 is a "typical" value for the flow velocity over the domain of interest. The ratio of the first to second term on the RHS of eq. (1.6) is the previously encountered magnetic Reynolds number

$$\mathrm{R}_m = \frac{u_0 \ell}{\eta} \tag{1.7}$$

The quantity R_m measures the relative importance of induction versus dissipation *over length scales of order* ℓ. One can then expect that in the limit $\mathrm{R}_m \gg 1$, induction by the flow dominates the evolution of $\mathbf{B}$, while in the opposite limit of $\mathrm{R}_m \ll 1$, induction makes a negligible contribution and $\mathbf{B}$

simply decays away under the influence of Ohmic dissipation. The distinction between these two physical regimes is meaningful as long as one can define a suitable R_m for the flow as a whole, which, in turn, implies that one can estimate, *a priori*, a length scale ℓ that will adequately characterize the evolving magnetic field at all time over the whole solution domain. As we proceed it will become clear that this is not always straightforward, or even possible.

1.1.4 Poloidal and toroidal magnetic fields

The observations reviewed in the preceding chapter indicate rather clearly that the Sun has a well-defined, large-scale magnetic component that is axisymmetric with respect to the rotation axis. In spherical polar coordinates (r, θ, ϕ), such a magnetic field can be written as

$$\mathbf{B}(r, \theta, t) = \nabla \times (A(r, \theta, t)\hat{\mathbf{e}}_\phi) + B(r, \theta, t)\hat{\mathbf{e}}_\phi; \tag{1.8}$$

Here the vector potential A defines the *poloidal* component of the field, i.e., a field contained in meridional ($[r, \theta]$) planes. The azimuthal component B is a *toroidal field*. Evidently eq. (1.8) satisfies the constraint $\nabla \cdot \mathbf{B} = 0$ identically. The advantage of this representation is that it allows to separate the (three component) induction equation (1.1) into *two* components for the scalar fields A and B. If one further assumes that the large scale flow $\mathbf{u}$ is also axisymmetric and is comprised of a large-scale *meridional circulation* $\mathbf{u}_p(r, \theta)$ (i.e., a flow contained in $[r, \theta]$ planes) and (differential) rotation $\varpi\Omega(r, \theta)$, one obtains

$$\frac{\partial A}{\partial t} = \varpi^{-1}\mathbf{u}_p \cdot \nabla(\varpi A) + \eta \left(\nabla^2 - \frac{1}{\varpi^2}\right) A \tag{1.9}$$

$$\frac{\partial B}{\partial t} = -\varpi\nabla\left(\frac{B\mathbf{u}_p}{\varpi}\right) + \varpi\mathbf{B}_p \cdot \nabla\Omega + \eta\left(\nabla^2 - \frac{1}{\varpi^2}\right) B + (\nabla\eta) \times (B\hat{\mathbf{e}}_\phi) \tag{1.10}$$

where $\varpi = r\sin\theta$ and $\mathbf{B}_p \equiv \nabla \times (A\hat{\mathbf{e}}_\phi)$ is a notational shortcut for the poloidal field.

On numerous occasions in this and subsequent chapters we will seek solutions to eqs. (1.9)–(1.10) inside a sphere (radius R) of magnetized fluid; in the "exterior" $r > R$ there is only vacuum, which implies vanishing electric currents[3]. In practice we will need to match whatever solution we compute in $r < R$ to a current-free solution in $r > R$; such a solution must satisfy

$$\frac{4\pi}{c}\mathbf{j} = \nabla \times \mathbf{B} = 0. \tag{1.11}$$

For an axisymmetric system such as considered here the current-free constraint (1.11) then translates into the requirement that

$$\nabla^2 (A(r,\theta,t)\hat{\mathbf{e}}_\phi) = 0, \tag{1.12}$$

$$B(r,\theta,t) = 0, \tag{1.13}$$

Whatever solution to eqs. (1.9)–(1.10) is computed within the sphere must then be smoothly matched to a solution of eqs. (1.12)–(1.13) in the exterior. In particular, the vector potential A must be continuous up to its first derivative normal to the surface, so that the magnetic field component tangential to the surface remains continuous across $r = R$. Regularity of the magnetic field on the symmetry axis requires that we set $B = 0$ there. Without any loss of generality, we can also set $A = 0$ on the axis.

1.2 Diffusive decays of magnetic fields [Sbdifuz]

After this lengthy preamble, it is time to get down to business. Before we try to come up with flows leading to field amplification, we better understand the enemy, namely magnetic field decay by Ohmic dissipation. Consequently, we first consider the evolution of magnetic fields in a conducting fluid, in the absence of any fluid motion (or, more generally, in the $\mathrm{R}_m \ll 1$ limit). The induction equation then reduces to

$$\frac{\partial \mathbf{B}}{\partial t} = \eta \nabla^2 \mathbf{B}, \tag{1.14}$$

where we have further assumed that the magnetic diffusivity η is constant throughout the spatial domain of interest. Were it not that we are dealing here with a vector —as opposed to scalar— quantity, this would look just like

[3]Well, as we learned in part I of the course, in the solar case the tenuous coronal gas is actually a pretty good conductor; however the nature of the outer boundary condition will not greatly influence the dynamo solutions we will be computing in subsequent chapters, so we'll stick to current-free boundary conditions.

a simple heat diffusion equation, with η playing the role of thermal diffusivity. Before attempting to formally solve this equation, let us first obtain an order-of-magnitude estimate for the timescale τ_η over which a magnetic field $\mathbf{B}$ with typical length scale ℓ can be expected to decay. Replacing $\partial/\partial t$ by and $1/\tau_\eta$ and ∇^2 by $1/\ell^2$, eq. (1.14) yields

$$\tau_\eta \sim \frac{\ell^2}{\eta}. \tag{1.15}$$

Now, for conditions typical of the solar interior we have $\eta \sim 10^3\,\mathrm{cm^2\,s^{-1}}$, so that the diffusive time scale for a large-scale field pervading the solar interior ($\ell \sim R_\odot \simeq 7\times 10^{10}$ cm) is $\tau \sim 10^{11}\,\mathrm{yr}$, i.e., longer than the main-sequence lifetime of the Sun. Note that this is due primarily to the large spatial scale of the system, as opposed to an exceedingly low diffusivity; a magnetic field within a one meter wide sphere of copper ($\eta \sim 10^5\,\mathrm{cm^2\,s^{-1}}$) would diffusively decay on a timescale $\tau \sim 0.1\,\mathrm{s}$! The *existence* of a solar magnetic field is then not really surprising; any large-scale fossil field present in the Sun's interior upon its arrival on the ZAMS would still be there today at almost its initial strength. The challenge in modeling the solar magnetic field is to reproduce the peculiarities of its spatial and temporal variations, in particular the cyclic variation of its large-scale component on a $\sim 22\,\mathrm{yr}$ timescale. But we are getting ahead of ourselves here. Back to simple resistive decay.

1.2.1 Reformulation as an eigenvalue problem

Let us now seek specific solutions to eq. (1.14), for a few situations of solar interest. One such situation is the resistive decay of a purely poloidal field pervading the solar interior. For this purpose it turns out to be convenient to work with the induction equation written in terms of the vector potential $\mathbf{A}$ which, for a purely poloidal field aligned with the polar axis, is simply

$$\mathbf{A}(r,\theta,t) = A(r,\theta,t)\hat{\mathbf{e}}_\phi \tag{1.16}$$

so that equation (1.9) reduces to

$$\frac{\partial A}{\partial t} = \eta\left(\nabla^2 - \frac{1}{\varpi^2}\right)A \tag{1.17}$$

For a constant magnetic diffusivity η, none of the PDE coefficients depend on either r, θ or t, so that we can seek solutions that are fully separable in r, θ, and t:

$$A(r,\theta,t) = a(r)b(\theta)\,e^{\lambda t} \tag{1.18}$$

1.2.2 Results for constant magnetic diffusivity

Tom rewrites this one

1.2.3 Results for a magnetic diffusivity varying with depth

We end this section by a brief examination of the diffusive decay of large-scale magnetic fields in the solar interior. The primary complication centers on the magnetic diffusivity, which not only is no longer constant throughout the domain, but also turns out to be rather difficult to compute from first principles[4]. To begin with, the depth variations of the temperature and density in a solar model lead to the magnetic diffusivity avrying from about $10^2\,\mathrm{cm}^2\,\mathrm{s}^{-1}$ in the central core to $\sim 10^4\,\mathrm{cm}^2\,\mathrm{s}^{-1}$ at the core-envelope interface. This variation is however dwarfed by the much larger increase in the net magnetic diffusivity expected in the turbulent environment of the convective core. We will look into this in some detail in chapter IV.4. For the time being let us simply take for granted that η is much larger in the envelope than in the core. Innorder to examine the consequences of this variation on the magnetic diffusive eigenmode, we consider a simplified situation whereby η assumes a constant value η_c in the core, a constant value η_e ($\gg \eta_c$) in the envelope, the transition occurring smoothly across a thin spherical layer coinciding with the core-envelope interface. This variation can be expressed as

$$\eta(r) = \eta_c + \frac{\eta_e - \eta_c}{2}\left[1 + \mathrm{erf}\left(\frac{r - r_c}{w}\right)\right], \tag{1.19}$$

where $\mathrm{erf}(x)$ is the error function, r_c is the radius of the core-envelope interface, and w is the half-width of the transition layer.

Even though we now have a r-dependency in η, the problem is still separable in θ and t. Consequently, all we have to solve is the 1D eigenvalue problem presented by

$$\lambda a(r,\theta) = \frac{1}{r^2}\frac{\partial}{\partial r}\left(\eta(r) r^2 \frac{\partial a}{\partial r}\right) - \eta(r)\frac{l(l+1)}{r^2} a, \qquad l = 1, 2, ... \tag{1.20}$$

where as before we have expressed all lengths in units of R, and time in units of the diffusion time (based on the envelope diffusivity η_e), so that the functional $\eta(r)$ appearing in eq. (1.20) is now dimensionless. We now seek numerical solutions, subjected to the boundary conditions $a(r = 0) = 0$

[4]See the bibliography at the end of this chapter for some references.

and smooth matching to a potential field solution in $r/R > 1$, with the diffusivity ratio $\Delta = \eta_c/\eta_e$ as a parameter of the model. Since we can make a reasonable guess at the eigenvalue on the basis of the diffusion time and adopted values of l and η_c, inverse iteration is the technique of choice.

Panels (A) through (C) of Figure 1.2.3 shows the slowest decaying poloidal eigenmodes for the diffusivity profile given by eq. (1.19) with $r_c/R = 0.7$ and $w/R = 0.05$, for diffusivity contrasts $\Delta\eta = 1$ (constant diffusivity), 10^{-1} and 10^{-3}. The corresponding eigenvalue (σ) is listed below each panel, in units of diffusion time based on the η_e. Panel (D) shows the corresponding radial eigenfunctions, together with the diffusivity profile for $\Delta\eta = 10^{-3}$. Notice how the eigenmodes are increasingly concentrated in the core region ($r/R \lesssim 0.7$) as $\Delta\eta$ decreases, i.e., they are "excluded" from the convective envelope. This is sometimes referred to in the literature as the *diamagnetic effect*. This effect is not restricted to purely diffusive systems, and has interesting consequences for models of the solar dynamo, something to be explored in a later chapter.

What is there to conclude from our study of the diffusive decay of magnetic fields ? Perhaps our most interesting results is the marked decrease of the diffusive decay time with increasing angular and radial degrees of the eigenmodes. For $n = 1$, going from $l = 1$ to $l = 2$ halves the decay time (see panels [A] and [B] on Fig. **??**); likewise for $l = 1$ in going from $n = 1$ to $n = 2$ (panels [A] and [E] on Fig. **??**). And remember, λ appears in an exponential (cf. eq. [1.18]), where factors of two go a long way. This means that left to decay long enough, any arbitrarily complex magnetic field in the Sun or stars will eventually end up looking dipolar[5].

There exists classes of early-type main-sequence stars, i.e. stars hotter and more luminous than the Sun and without deep convective envelope, that are believed to contain strong, large-scale fossil magnetic fields left over from their contraction toward the main-sequence (see §1.1 in the previous chapter). The slowly rotating, chemically peculiar Ap stars are the best studied class of such objects. Reconstruction of their surface magnetic field distribution suggests almost invariably that the fields are largely dominated by the dipole component, as one would have expected from the preceding discussion if the observed magnetic fields have been diffusively decaying for tens or hundreds of millions of years[6].

---

[5] Is this always true? Can you think of circumstances where this would not be the case?

[6] Care is warranted in making such conclusions on the basis of stellar observations, as the current techniques used to infer the presence and structure of the surface fields, based on Zeeman splitting and/or polarization of starlight, are significant biased towards the

1.3 Magnetic field evolution in a cellular flow [Sbadvec]

Having now investigated in some the details the resistive decay of magnetic field, we turn to the other physical mechanism embodied in eq. (1.1): growth of the magnetic field in response to the inductive action of a flow $\mathbf{u}$. We first take a quick look at field amplification in an idealized model, and then move on to a specific example using a "real" flow.

1.3.1 Hydrodynamical stretching and field amplification

Let's revert for a moment to the ideal MHD case ($\eta = 0$). The induction equation can then expressed as

$$\frac{\partial \mathbf{B}}{\partial t} + (\mathbf{u} \cdot \nabla)\mathbf{B} = \mathbf{B} \cdot \nabla \mathbf{u}, \tag{1.21}$$

where it was further assumed that the flow is incompressible ($\nabla \cdot \mathbf{u} = 0$). The LHS of eq. (1.21) is the Lagrangian derivative of $\mathbf{B}$, expressing the time rate of change of $\mathbf{B}$ in a fluid element moving with the flow. The RHS expresses the fact that this rate of change is proportional to the local *shear* in the flow field. Shearing has the effect of *stretching* magnetic fieldlines, which is what leads to magnetic field amplification.

As a simple example, consider on Figure 1.3.1 a cylindrical fluid element of length L_1, threaded by a magnetic field parallel to the axis of the cylinder, imbedded in a perfectly conducting incompressible fluid and subjected to a stretching motion ($\partial u_x/\partial x > 0$) along its central axis such its length increases to L_2. Mass conservation demands that $R_2/R_1 = \sqrt{L_1/L_2}$. Conservation of the magnetic flux ($= \pi R^2 B$) in turn leads to

$$\frac{B_2}{B_1} = \frac{L_2}{L_1} \tag{1.22}$$

i.e., the field strength is amplified in direct proportion to the level of stretching. This almost trivial result is in fact at the very heart of *any* magnetic field amplification in the magnetohydrodynamical context, and illustrates two crucial aspects of the mechanism: first, this works only if the fieldlines are frozen into the fluid, i.e., in the high magnetic Reynolds number regime. Second, mass conservation plays an essential role here; the stretching motion along the tube axis *must* be accompanied by a compressing fluid motion

lower multipoles because the stellar surface remains spatially unresolved.

perpendicular to the axis if mass conservation is to be satisfied. It is this latter compressive motion, occurring perpendicular to the magnetic fieldlines forming the flux tube, that is ultimately responsible for field amplification; the horizontal motion occurs parallel to the magnetic fieldline, and so cannot in itself have any inductive effect as per eq. (1.1)[7].

The challenge, of course, is to realize this idealized scenario in practice, i.e., to find a flow which achieves the effect illustrated on Figure 1.3.1. With magnetic dissipation brought back to the picture, another important effect must be taken into consideration. Since field amplification by stretching involves a decrease in the radius R of the flux tube, eventually there will come a time where R has become so small that the effective local Reynolds number based on the tube radius ($\ell = R$ in eq. (1.7)) is of order unity, so that magnetic dissipation prevents any further amplification of the magnetic field. Make a mental note of this concept of decreasing length scale, as it will come back to haunt us again and again.

insert sub§on VZ STF rope dynamo here?

1.3.2 A cellular flow solution

We are now ready to some actual calculations using the full induction equation! In Cartesian geometry, we consider the action of a steady, incompressible ($\nabla \cdot \mathbf{u} = 0$) two-dimensional flow

$$\mathbf{u}(x, y) = u_x(x, y)\hat{\mathbf{e}}_x + u_y(x, y)\hat{\mathbf{e}}_y \tag{1.23}$$

on a two-dimensional magnetic field

$$\mathbf{B}(x, y, t) = B_x(x, y, t)\hat{\mathbf{e}}_x + B_y(x, y, t)\hat{\mathbf{e}}_y \tag{1.24}$$

Note that neither the flow nor the magnetic field have a z-component, and that their x and y-components are both independent of the z-coordinate. The flow is said to be *planar* because $u_z = 0$, and has an ignorable coordinate (i.e., translational symmetry) since $\partial/\partial z \equiv 0$ for all field and flow components. You should convince yourself that such a magnetic field can be represented by the vector potential

$$\mathbf{A} = A(x, y, t)\hat{\mathbf{e}}_z. \tag{1.25}$$

and that under this representation, lines of constant A in the $[x, y]$ plane coincide with magnetic fieldlines, and furthermore that a given value of A

[7] Hold it now, how do you reconcile this statement with eq. (1.22), which indicates rather unambiguously that one can have $\partial\mathbf{B}/\partial t > 0$ with $\mathbf{B} = B_x\hat{\mathbf{e}}_x$ and $\mathbf{u} = u_x(x)\hat{\mathbf{e}}_x$?

uniquely labels a single fieldline. The only non-trivial component of the induction equation (1.3) is its z-components, which takes the form

$$\frac{\partial A}{\partial t} = -\mathbf{u} \cdot \nabla A + \eta \nabla^2 A. \tag{1.26}$$

This is a linear advection-diffusion equation, describing the transport of a passive scalar quantity A by a flow $\mathbf{u}$, and subject to diffusion, the magnitude of which being measured by η. In view of the symmetry and planar nature of the flow, it is convenient to write the 2-D flow field in terms of a *stream function* $\Psi(x,y)$:

$$\mathbf{u}(x,y) = u_0 \left(\frac{\partial \Psi}{\partial y} \hat{\mathbf{e}}_x - \frac{\partial \Psi}{\partial x} \hat{\mathbf{e}}_y \right) \tag{1.27}$$

It is easily verified that any flow so defined will identically satisfy the condition $\nabla \cdot \mathbf{u} = 0$. As with eq. (1.25), a given numerical value of Ψ uniquely labels one streamline of the flow. Consider now the stream function

$$\Psi(x,y) = \frac{L}{4\pi} \left(1 - \cos\left(\frac{2\pi x}{L} \right) \right) \left(1 - \cos\left(\frac{2\pi y}{L} \right) \right), \qquad x, y \in [0, L] \tag{1.28}$$

This describes a counterclockwise cellular flow centered on $(x,y) = (L/2, L/2)$, as shown on Figure 1.3.2. The maximal velocity amplitude $_{\max}\|\mathbf{u}\| = u_0$ is found along the streamline $\Psi = u_0 L/(2\pi)$, plotted as a thicker line on Figure 1.3.2. This streamline is well approximated by a circle of radius $L/4$, and its streamwise circulation period turns out to be $1.065\pi L/2u_0$, quite close to what one would expect in the case of a perfectly circular streamline. In what follow this timescale is denoted $\tau_{\rm c}$ and referred to as the *turnover time* of the flow. Note that both the normal and tangential components of the flow vanish on the boundaries $x = 0, L$ and $y = 0, L$. This implies that the domain boundary is itself a streamline ($\Psi = 0$, in fact), and that every streamline interior to the boundary closes upon itself within the spatial domain bounded by the $\Psi = 0$ streamline. These (simple) topological properties of the flow defined by eqs. (1.27) and (1.28) may seem largely irrelevant at this stage of our inquiries, but later chapters will reveal that they are in fact crucial to the dynamo problem.

We now investigate the inductive action of this flow by solving a nondimensional version of eq. (1.26), by expressing all lengths in units of L, and time in units of L/u_0, so that

$$\frac{\partial A}{\partial t} = -\frac{\partial \Psi}{\partial y}\frac{\partial A}{\partial x} + \frac{\partial \Psi}{\partial x}\frac{\partial A}{\partial y} + \frac{1}{\mathrm{R}_m}\left(\frac{\partial^2 A}{\partial x^2} + \frac{\partial^2 A}{\partial y^2} \right) \qquad x, y \in [0, L] \tag{1.29}$$

where $\mathrm{R}_m = u_0 L/\eta$ is the magnetic Reynolds number for this problem, and the corresponding diffusion time is then $\tau_\eta = \mathrm{R}_m$ in dimensionless units. Equation (1.29) is solved as an initial-boundary value problem in two spatial dimensions, with spatial and temporal derivatives both evaluated using second-order centered finite differences (see boxes XX and YY). All calculations described below start at $t = 0$ with an initially uniform, constant magnetic field $\mathbf{B} = B_0 \hat{\mathbf{e}}_x$, equivalent to:

$$A(x, y, 0) = B_0\, y, \tag{1.30}$$

We consider a situation where the magnetic field normal to the boundaries is held fixed, which amounts to holding the vector potential fixed on the boundary[8]. Figure 1.3.2 shows the variation with time of the magnetic energy , computed via eq. (1.5), for four solutions having $\mathrm{R}_m = 10, 10^2, 10^3$ and 10^4. Figure 1.3.2 shows the evolving shape of the magnetic fieldlines in the $\mathrm{R}_m = 10^3$ solution at 9 successive epochs[9]. The solid dots are "floaters", namely Lagrangian markers moving along with the flow. At $t = 0$ all floaters are equidistant and located on the fieldline initially coinciding with the coordinate line $y/L = 0.5$, that (evolving) fieldline being plotted as a thicker line on all panels. Figure 1.3.2 covers two turnover times, and the corresponding times are marked by solid dots on the $\mathrm{R}_m = 10^3$ curve on Fig. 1.3.2.

The solid dots are not there yet on Fig.1.3.2.

The behavior of the energy curve is noteworthy; at first, the magnetic energy increases quadratically in time. This is precisely what one would expect from the shearing action of the flow on the initial B_x-directed magnetic field, which leads to a growth of the B_y-component that is linear in time. However, for $t/\tau_c \gtrsim 2$ the magnetic energy starts to decrease again and eventually ($t/\tau_c \gg 1$) levels off to a constant value. To understand the origin of this behavior we need to turn to Figure 1.3.2 and examine the solutions in some detail.

The counterclockwise shearing action of the flow is quite obvious on Fig. 1.3.2 in the early phases of the evolution, leading to a rather pretty spiral pattern as magnetic fieldlines get wrapped around one another. Note that the distortion of magnetic fieldlines by the flow implies a great deal of *stretching* in the streamwise direction. This is most obvious upon noting that the distance between adjacent floaters increases monotonically in time. It is no accident that the floaters end up in the regions of maximum field amplification on frames 2—5; they are initially positioned on the fieldline

[8]Can you figure that one out?

[9]An animation of this evolving solution can be viewed on the course Web Page.

coinciding with the line $y = L/2$, initially everywhere perpendicular to the shearing flow (see Fig. 1.3.2), which pretty much ensures maximal inductive effect, as per eq. (1.26). The fact that all floaters remain at first "attached" onto their original fieldline is what one would have expected from the fact that this is a relatively high-R_m solution, so that flux-freezing is effectively enforced. As the evolution proceeds, the magnetic field keeps increasing in strength, but is more and more confined to spiral "sheet" regions of decreasing thickness.

By the time we hit one turnover time ($\tau_c = 0.532\pi$ in our dimensionless units, corresponding approximately to frame 5 on Fig. 1.3.2), it seems that we are making progress towards our goal of producing a dynamo; we have a flow field which, upon acting on a preexisting magnetic field, has intensified the strength of that field, at least in some localized regions of the spatial domain. However, beyond $t \sim \tau_c$ the sheets of magnetic fields are gradually disappearing, first near the center of the flow cell (frames 5—7), and later everywhere except close to the domain boundaries (frames 7—9). Notice also how, from frame 5 onward, the floaters are seen to "slip" off their original fieldlines, indicating that diffusion is taking place. Yet, we evidently still have $t \ll \tau_\eta$ ($\equiv \mathrm{R}_m = 10^3$ here), which would normally suggest that diffusion has not yet had enough time to significantly affect the solution. What is going on here?

The solution to this apparent dilemma lies with the realization that we have defined R_m in terms of the global length scale L characterizing the flow. This was a perfectly sensible thing to do on the basis of the flow configuration and initial condition on the magnetic field. However, as the evolution proceeds beyond $\sim \tau_c$ the decreasing thickness of the magnetic field sheets means that the global length scale L is no longer an adequate measure of the "typical" length scale of the magnetic field, which is what is needed to estimate the diffusion time τ_η (see eq. (1.15)). Figure 1.3.2 shows a series of cuts of the vector potential A in a $\mathrm{R}_m = 10^4$ solution, plotted along the coordinate line $y = L/2$, at equally spaced successive time intervals covering two turnover times. Clearly the inexorable winding of the fieldline leads to a general decrease of the length scale characterizing the evolving solution. In fact, each turnover time adds two new "layers" of alternating magnetic polarity to the spiraling sheet configuration, so that the average length scale ℓ decreases as t^{-1}:

$$\frac{\ell(t)}{L} \propto \frac{L}{u_0 t}. \tag{1.31}$$

which implies that the *local* dissipation time is also decreasing as t^{-1}. On the other hand, examination of Fig. 1.3.2 soon reveals that the (decreasing) length scale characterizes the thickness of elongated magnetic structures that are themselves more or less *aligned* with the streamlines, so that the turnover time τ_c remains the proper timescale measuring field induction. With τ_c so fixed and τ_η inexorably decreasing, the solution is bound to reach a point where $\tau_\eta \simeq \tau_c$, *no matter how small dissipation actually is.* To reach that stage just takes longer in the higher R_m solutions, since more winding of the fieldlines is needed. Larger magnetic energy can build up in the transient phase, but the growth of the magnetic field is *always* arrested. Equating τ_c ($\equiv L/u_0$) to the *local* dissipation time ℓ^2/η, one readily finds that the length scale ℓ at which both process become comparable can be expressed in terms of the *global* R_m as

$$\frac{\ell}{L} = (\mathrm{R}_m)^{-1/2}, \qquad \mathrm{R}_m = \frac{u_0 L}{\eta}. \tag{1.32}$$

That such a balance between induction and dissipation materializes means that a steady-state can be attained. Figure 1.3.2 shows four such steady states solutions for increasing values of the (global) magnetic Reynolds number R_m. The higher R_m solutions clearly show *flux expulsion* from the central regions of the domain. This is a general feature of steady, high-R_m magnetized flows with closed streamlines: magnetic flux is expelled from the regions of closed streamlines towards the boundaries of the flow cells, where it ends up concentrated in layers which indeed have a thickness of order $\mathrm{R}_m^{-1/2}$, as suggested by eq. (1.32). It is important to understand how and why this happens.

1.3.3 Flux expulsion

To first get an intuitive feel for how flux expulsion operates, go back to Figure 1.3.2. As the flow wraps the fieldlines around one another, it does so in a manner that folds fieldlines of opposite polarity closer and closer to each other. You may convince yourself that this is the case by adding arrows to the fieldlines, starting with uniformly right-pointing arrows on the first panel, and carefully following where those arrow are pointing in subsequent frames, a bit like some directional Lagrangian markers. When two magnetic fieldlines of opposite polarities are squeezed closer together than the dissipative length scale (eq. [1.32]), resistive decay takes over and destroys the field faster than it is being stretched. The magnetic fieldlines are experiencing *destructive folding.* This can only be avoided along the boundaries, where the normal component of the field is being held fixed. For flux expulsion to operate, the magnetic Reynolds number must be high enough for the fieldlines to be dragged by the flow, i.e., for flux-freezing to be effectively enforced. Otherwise the field is largely insensitive to the flow, and fieldlines are hardly deformed with respect to their initial configuration (as on panel [A] of Fig. 1.3.2).

Consider now the implication for the total magnetic flux across the domain; flux conservation requires that the normal flux B_0L imposed at the right and left boundaries must somehow cross the interior; because of flux expulsion, it can only do does so in the thin layers along the bottom and top boundaries. Since the thickness of these layers scales as ${\rm R}_m^{-1/2}$, it follows that the field strength therein scales as $\sqrt{{\rm R}_m}$, which in turn implies that the total magnetic energy in the domain scales also as $\sqrt{{\rm R}_m}$ in the $t \gg \tau_c$ limit [10].

Flux expulsion is believed to be in part responsible for the observed accumulation of magnetic fields at the boundaries of supergranulation cells on the solar surface.

1.3.4 Digression: the electromagnetic skin depth

There is far more to flux expulsion than meets the eye, and we are far from done exploring consequences of this mechanism. Let's firat launch into what will first appear to be an unrelated digression. Working in cartesian coordinates, consider a flat plate coinciding with the xz-plane, with the semi-infinite space right of the plate ($y > 0$) containing a conducting material of constant magnetic resistivity η. At $t = 0$ an oscillating, y-directed magnetic field $\mathbf{B} = B\hat{\mathbf{e}}_y$ is turned on at the boundary:

$$B(y, 0) = 0, \tag{1.33}$$

$$B(0, t) = B_0 \cos(\omega t). \tag{1.34}$$

The magnetic field evolution in $y > 0$ is governed by the y-component of the induction equation (with $\mathbf{u} = 0$), which here reduces to

$$\frac{\partial B}{\partial t} = \eta \frac{\partial^2 B}{\partial y^2}, \tag{1.35}$$

This PDE is readily solved by Laplace Transform. The transformed eq. (1.35) is

Ref to Laplace TRansform here

$$sf = \eta \frac{\partial^2 f}{\partial y^2} \tag{1.36}$$

which admits solutions in the form:

$$f(y,s) = c_1 \exp(-\sqrt{s/\eta}y) + c_2 \exp(\sqrt{s/\eta}y) \tag{1.37}$$

The transformed boundary condition is

$$f(0,s) = B_0 \int_0^\infty dt \mathrm{e}^{-st} \cos(\omega t) = \frac{B_0 s}{s^2+\omega^2}. \tag{1.38}$$

Regularity of the solution for $y \to \infty$ requires $c_2 = 0$, so that the solution is

$$f(y,s) = \frac{B_0 s}{s^2+\omega^2} \exp(-\sqrt{s/\eta}y) \tag{1.39}$$

You now go to your favorite Tables of Laplace Transforms, which lists the inverse transform of eq. (1.39) to be

$$B(y,t) = \exp(-\sqrt{\omega/2\eta}y)\cos(\omega t - \sqrt{\omega/2\eta}y) - \frac{1}{\pi}\int_0^\infty \mathrm{e}^{-ut}\sin(\sqrt{\eta u})\frac{u}{u^2+\omega^2}\mathrm{d}u \tag{1.40}$$

Now that integral on the RHS looks nasty... however in the limit of large t, the integrand vanishes exponentially. Physically, it corresponds to the transient induced by abruptly turning on the field at $t = 0$[11]. Consequently, a good asymptotic approximate solution is

$$B(y,t) \simeq \exp(-\sqrt{\omega/2\eta}y)\cos(\omega t - \sqrt{\omega/2\eta}y) \qquad [t \text{ large}] \tag{1.41}$$

This describes an oscillating field, but with an amplitude decaying with y exponentially[12]. The corresponding length scale for the amplitude is

$$\ell = \sqrt{\frac{2\eta}{\omega}} \tag{1.42}$$

[10] Hold it, $\mathcal{E}_\mathrm{B} \propto \mathbf{B}^2$ as per eq. (1.4); how can the magnetic field strength and magnetic energy *both* scale as $\sqrt{\mathrm{R}_m}$?

[11] So why didn't I simply pick a $\sin(\omega t)$ dependence for the boundary condition? That wouldn't have any transient? Or would it? Try it and see if you can work out the resulting inverse Laplace transform...

[12] An "animation" of equation (1.41) can be viewed on the course Web Page.

and is called the *electromagnetic skin depth*[13].

So why this digression? Well, go back to the cellular flow and imagine that you are an observed located in the center of the flow cell, looking at the domain boundaries while rotating with angular velocity u_0/L; what you "see" in front of you is an "oscillating" magnetic field, in the sense that it flips sign with "angular frequency" u_0/L. The corresponding electromagnetic skin depth would then be

$$\frac{\ell}{L} = \sqrt{\frac{2\eta}{u_0 L}} == \sqrt{\frac{2}{\mathrm{R}_m}}. \tag{1.43}$$

which corresponds to the thickness of the "boundary layer" where significant magnetic field is present in the steady-states shown on Figure 1.3.2. How about this for a mind flip...

1.3.5 Timescales for field amplification and decay

Back to our cellular flow. Flux expulsion or not, it is clear from Figure 1.3.2 (solid lines) that some level field amplification has occurred in the high R_m solutions, in the sense that $\mathcal{E}_B(t \to \infty) > \mathcal{E}_B(0)$. But is this a dynamo? The solutions of Fig. 1.3.2 have strong electric currents in the direction perpendicular to the plane of the paper, and these currents are subjected to resistive dissipation. Have we then reached the goal stated at the beginning of the chapter, namely, to amplify and maintain a weak, preexisting magnetic field against Ohmic dissipation?

In a narrow sense yes, but a bit of reflection will show that the boundary conditions are playing a crucial role; The only reason that the magnetic energy does not asymptotically go to zero is that the normal field component is held fixed at the boundaries, which, in the steady-state, implies a non-zero Poynting flux into the domain across the left and right vertical boundaries. The magnetic field is not avoiding resistive decay because of field induction within the domain, but rather because external energy (and magnetic flux) is being pumped in through the boundaries. This is precisely what is embodied in the second and third terms on the RHS of eq. (1.5).

What if this were not the case? One way to work around the boundary problem is to replace the fixed flux boundary conditions by periodic

[13]Equation (1.42) can actually be derived by a very simple order-of-magnitude argument; go back to §II.5.1 and try to figure it out.

boundary conditions:

$$A(x,0) = A(x,L), \qquad A(0,y) = A(L,y). \tag{1.44}$$

There is still a net flux across the vertical boundary at $t = 0$, but the boundary flux is now free to decay away along with the solution. You get to compute such a solution in Problem 2.3. It is time to reveal that the hitherto unexplained dotted lines on Fig. 1.3.2 correspond in fact to solutions computed with such boundary conditions, for the same cellular flow and initial condition as before.

Evidently the magnetic energy now decays to zero, confirming that the boundaries indeed played a crucial role in the sustenance of the magnetic field in our previous solutions. What is noteworthy is the rate at which it does so. In the absence of the flow and with freely decaying boundary flux, the initial field would diffuse away on a timescale $\tau_\eta \sim L^2/\eta$, which is equal to R_m if we retain the scaling of τ in terms of L/u_0. With the flow turned on, the decay proceeds at an accelerated rate because of the inexorable decrease of the typical length scale associated with the evolving solution, which we argued in §**??** varied as t^{-1}. What then is the typical timescale for this enhanced dissipation? The decay phase of the field (for $t \gg L/u_0$) is approximately described by

$$\frac{\partial A}{\partial t} = \eta \nabla^2 A, \tag{1.45}$$

An estimate for the dissipation timescale can be obtained once again by dimensional analysis, by replacing ∇^2 by $1/\ell^2$, as in §1.2 with the important difference that ℓ is now a function of time:

$$\ell \to \ell(t) = \left(\frac{L}{t}\right)\left(\frac{L}{u_0}\right) \tag{1.46}$$

from our previous discussion (cf. Fig.1.3.2 and accompanying text). This leads to

$$\frac{\partial A}{\partial t} \simeq -\frac{\eta U^2 t^2}{L^4} A, \tag{1.47}$$

where the minus sign is introduced in view of the fact that $\nabla^2 A < 0$ in the decay phase. Equation (1.47) integrates to

$$\frac{A(t)}{A_0} = \exp\left[-\frac{\eta U^2}{3L^4} t^3\right] = \exp\left[-\frac{1}{3\mathrm{R}_m}\left(\frac{U^3 t^3}{L^3}\right)\right]. \tag{1.48}$$

Equation (1.48) indicates that with t measured in units of L/u_0, the decay time scales as $\mathrm{R}_m^{1/3}$. This is indeed a remarkable situation: in the low magnetic diffusivity regime (i.e., high R_m), the flow has in fact *accelerated* the decay of the magnetic field, even though large field intensification can occur in the early, transient phases of the evolution. This is not at all what a dynamo should be doing! Let this exemplify an important warning in the dynamo game. Before claiming that this or that flow can act as a dynamo, it is important to ensure that the evolution of the system has been followed over many times the characteristic timescale of the flow.

As it turns out, flux expulsion is even trickier than the foregoing discussion may have led you to believe! What flux expulsion does is destroy the mean magnetic field component directed *perpendicular* to the flow streamlines. It cannot do a thing to a mean component oriented *parallel* to streamlines. For completely general flow patterns and initial conditions, the dissipative phase with timescale $\propto \mathrm{R}_m^{1/3}$ actually characterizes the approach to a state where the advected trace quantity —here the vector potential A— becomes constant *along each streamline*, with the corresponding constant value of A equal to the initial value of A averaged on each of those streamlines. For the cellular flow and initial conditions used above, this average turns out to be $\bar{A} = 0.5$ *for every streamline*, so that the $\mathrm{R}_m^{1/3}$ decay phase corresponds to the true decay of the magnetic field to zero amplitude. If $\bar{A}$ varies from one fieldline to the next, however, the $\mathrm{R}_m^{1/3}$ phase is followed by a third decay phase, which proceeds on a timescale $\sim \mathrm{R}_m$, since induction no longer operates ($\mathbf{u} \cdot \nabla A = 0$) and the typical length scale for A is once again L. You get to explore this phenomenon in problem 2.4 [14].

Always remember that all of this stuff pertains to high R_m fluids; here "high" typically means $\mathrm{R}_m \gtrsim 10^2$, not just $\mathrm{R}_m > 1$. At any rate, even with a more "favorable" initial condition we have further delayed field dissipation, but we still don't have a dynamo since dissipation will proceed inexorably, on the "long" timescale $\mathrm{R}_m(L/u_0)$.

1.3.6 Axisymmetrization by differential rotation

The simple cellular flow we have considered is reminescent of washing machines far more than of astrophysical bodies. In fact there exists a direct spherical equivalent of flux expulsion that might be quite relevant to the

[14] In case you're too lazy to do the problem, you can view an animation of this solution on the Course Home Page. But please do the problem anyway.

Sun, and to at least one other astronomical object which you probably did not expect to hear much about in these pages.

Working in spherical polar coordinates, we consider a sphere (radius R) of electrically conducting fluid, in a state of steady, axisymmetric differential rotation, with the angular velocity $\Omega(r,\theta)$ defined by the following parametrization:

$$\Omega(r,\theta)=\Omega_C+\frac{1}{2}\left[1+\mathrm{erf}\left(\frac{r-r_C}{w}\right)\right](\Omega_S(\theta)-\Omega_C), \tag{1.49}$$

where

$$\Omega_S(\theta)=\Omega_{Eq}(1-a_2\cos^2\theta-a_4\cos^4\theta) \tag{1.50}$$

is the surface latitudinal differential rotation. Figure 1.3.6 shows a 2D helioseismic inversion of the solar internal rotation, together with the differential rotation profile $\Omega(r,\theta)$ generated using eq. (1.49)–(1.50) with parameter values $\Omega_C/2\pi=432.8\,\mathrm{nHz}$, $\Omega_{Eq}/2\pi=460.7\,\mathrm{nHz}$, $a_2=0.1264$, $a_4/2\pi=0.1591$, $r_c=0.713R$, and $w=0.05R$. The degree of similarity with the "real" Sun is sufficient for our present purposes. Note in particular that both profiles are characterized by:

1. A convective envelope where the shear is predominantly in the latitudinal direction, with equatorial acceleration;

2. A deep core that rotates essentially rigidly, at a rate equal to that of the surface mid-latitudes;

3. A matching of the core and envelope rotation profiles occurring across a thin spherical layer located at the base of the convective envelope, so that strong radial shears exist in the polar and equatorial regions.

A measure of the turnover time for this problem is the differential rotation timescale

$$\tau_\mathrm{c}\equiv\frac{2\pi}{\Omega_{Eq}}(a_2+a_4)^{-1} \tag{1.51}$$

defined as the time required for a fluid element located at $r/R=1$ in the equatorial plane to perform a full revolution with respect to a fluid element located in the surface polar regions. The quantity $2\pi R/\tau_\mathrm{c}$ then becomes the measure of flow speed used to define the magnetic Reynolds number.

We seek a solution of the induction equation describing the (kinematic) evolution of a magnetic field pervading this fluid sphere, the field having initially the form of an dipole sith its syjmmetry axis is inclined by an angle Θ with respect to the rotation axis ($\theta = 0$). Such a magnetic field can be expressed in terms of a vector potential having components:

$$A_r(r, \theta, \phi) = 0 \tag{1.52}$$

$$A_\theta(r, \theta, \phi) = (R/r)^2 \sin\Theta(\sin\beta\cos\phi - \cos\beta\sin\phi) \tag{1.53}$$

$$A_\phi(r, \theta, \phi) = (R/r)^2[\cos\Theta\sin\theta - \sin\Theta\cos\theta(\cos\beta\cos\phi + \sin\beta\sin\phi)] \tag{1.54}$$

where β is the angle between the $\phi = 0$ plane, and the plane defined by the dipole and coordinate axes.

Equations (1.52)–(1.53) indicate that the vector potential for an inclined dipole can be written as the sum of two contributions, the first corresponding to a dipole ($\mathbf{A} \to A(r, \theta)\hat{\mathbf{e}}_\phi = (R/r)^2 \sin\theta$) aligned with the symmetry axis of the spherical coordinate system, the second to a perpendicular dipole (all terms proportional to $\sin\Theta$), their relative magnitude being equal to $\tan\Theta$[15]. Since the governing equation is linear, the solution for an inclined dipole can be broken into two independent solutions, one for the aligned dipole and the other for the perpendicular dipole. The solution for a perpendicular dipole is in many way similar to the cellular flow problem of §1.3. You can see how this may be the case by imagining looking from above onto the equatorial plane of the sphere; the fieldlines contained in that plane will have a curvature and will cross a circular boundary, yet topologically the situation is similar to the cellular flow studied in the preceding section: the (sheared) flow in the equatorial plane is made of closed, circular streamlines contained within that plane, so that we can expect flux expulsion to occur. For a freely decaying dipole in the high R_m regime,, the perpendicular component of the initial dipole is subjected to flux expulsion, and dissipated away, on a timescale ($\propto \mathrm{R}_m^{-1/3}$) much shorter than for purely diffusive decay limit, as demonstrated in §1.3. This leaves behind the aligned dipole, which itself decays on the "long" diffusive timescale ($\propto \mathrm{R}_m$).

But here is the amusing thing; for an observer looking at the magnetic field at the surface of the sphere, the enhanced decay of the perpendicular

[15]Can you work out the corresponding vector potential components? Can you also do it for an inclined quadrupole?

component of the dipole translates into a gradual decrease in the inferred tilt axis of the dipole. Figure 1.3.6 shows this effect, for the differential rotation profile given by eq. (1.49) and a magnetic Reynolds number $\mathrm{R}_m = 10^3$. Contours of constant B_r are plotted on the surface $r/R = 1$, with the neutral line ($B_r = 0$) plotted as a thicker line. At $t = 0$ the field has the form of a pure dipole tilted by $\pi/3$ with respect to the coordinate axis, and the sphere is oriented so that the observer (you!) is initially looking straight down the magnetic axis of the dipole. Advection by the flow leads to a distorsion of the initial field, with the subsequent buildup of small spatial scales in the r- and $\theta-$directions[16]. Note the winding and folding of the B_r-isocontours, so that large magnetic field gradients build up in the θ- and ϕ-direction (panels (B)–(F) on Fig. 1.3.6) Beyond about four turnover times ($t/\pi = 4$), the solution looks pretty much like a slightly inclined dipole whose tilt decreases steadily with time (panels (G)–(I)). So in a differentially rotating fluid system with high R_m, flux expulsion leads to the axisymmetrization of any non-axisymmetric magnetic field component initially present —or contemporaneously generated.

The efficiency of this symmetrization process should make us a little cautious in assuming that the large-scale magnetic field of the Sun, which one would deem roughly axisymmetric upon consideration of surface things like the sunspot butterfly diagram, is characterized by the same level of axisymmetry in the deep-seated generating layers, where the dynamo is presumed to operate. After all, standing in between is a thick, axisymmetrically differentially rotating convective envelope that must be reckoned with. In fact, we saw in §1.4 that observations of coronal density structures in the descending phase of the solar cycle can be interpreted in terms of a large-scale, tilted dipole component, with the tilt angle steadily decreasing over 3—4 years towards solar minimum. Interestingly, the differential rotation timescale for the Sun is ~ 6 months. Are we seeing the axisymmetrization process in operation? Axisymmetry is certainly a very convenient modeling assumption when working on the large scales of the solar magnetic field, but it may be totally wrong.

As it turns out, there exists considerable evidence that this process is operating, of all places, in the interior of the planet Saturn. Saturn's surface magnetic field is highly unusual among planetary magnetic fields, in that (1) it is almost perfectly dipolar, and (2) the axis if its dipole lies within one

[16]An animation of this solution, as well as a few others for different R_m and/or tilt angle, can be viewed on the course Web Page.

degree of the polar axis. Saturn also has the strongest zonal jets of all giant planets, and at least some dynamical models suggest this observed zonal flow is a surface manifestation of deep-seated differential rotation pervading the molecular H envelope of Saturn, outside of its metallic H core, and that this differential is characterized by constant angular velocity on cylinders centered about the rotation axis. Calculations of the symmetrization process show that for $\mathrm{R}_m \gtrsim 10^3$ outside the metallic H core, the surface field is efficiently symmetrized after 3—4 differential rotation timescales, even if the magnetic field is strongly non-axisymmetric at the core-envelope interface.

1.4 Some anti-dynamo theorems [Santidyn]

The cellular flow studied in §1.3, although it initially looked encouraging (cf. Fig. 1.3.2), proved not to be a dynamo after all. Is this peculiar to the flow defined by eqs. (1.27)–(1.28), or is this something more general? Exhaustively testing for dynamo action in all possible kinds of flow geometries is clearly impractical. However, it turns out that one can rule out *a priori* dynamo action in many classes of flows. These proofs are known in the literature as *anti-dynamo theorems.*

We first consider a powerful anti-dynamo theorem due to Ya. B. Zeldovich. The theorem rules out dynamo action in steady *planar flows* in cartesian geometry, i.e., flows of the form

$$\mathbf{u}_2(x,y,z) = u_x(x,y,z)\hat{\mathbf{e}}_x + u_y(x,y,z)\hat{\mathbf{e}}_y \tag{1.55}$$

in a bounded volume V at the boundaries (∂V) of which the magnetic field vanishes. Note that no restrictions are placed on the magnetic field, which can depend on all three spatial coordinate as well as time. Nonetheless, in view of eq. (1.55) is will prove useful to consider separately the z-component of the magnetic field $B_z(x,y,z,t)$ from the (2D) field component in the $[x,y]$ plane (hereafter denoted $\mathbf{B}_2$). It is readily shown that the z-component of the induction equation then reduces to

$$\frac{\partial B_z}{\partial t} + \mathbf{u}\cdot\nabla B_z = \eta\nabla^2 B_z \tag{1.56}$$

for spatially constant magnetic diffusivity. Now, the LHS is just a Lagrangian derivative, yielding the time variation of B_z as one moves along with the fluid. Multiplying this equation by B_z and integrating over V yields, after judicious use of a suitable vector identity and of the divergence theorem:

$$\frac{1}{2}\int_V \frac{\mathrm{D}B_z^2}{\mathrm{D}t}dV = \int_{\partial V} B_z(\nabla B_z)\cdot\mathbf{n}dS - \eta\int_V (\nabla B_z)^2 dV \tag{1.57}$$

Now, the first integral on the RHS vanishes since $\mathbf{B} = 0$ on ∂V by assumption. The second integral is positive definite, *therefore B_z always decays on the diffusive timescale* (cf. §1.2).

Consider now the magnetic field $\mathbf{B}_2$ in $[x, y]$ planes. The most general such 2D field can be written as the sum of a solenoidal and potential component:

$$\mathbf{B}_2(x, y, z, t) = \nabla\times(A\hat{\mathbf{e}}_z) + \nabla\Phi \tag{1.58}$$

where the vector potential A and scalar potential Φ both depend on all three spatial coordinates and time. Evidently, the constraint $\nabla\cdot\mathbf{B} = 0$ implies

$$\nabla_2^2\Phi = -\frac{\partial B_z}{\partial z} \tag{1.59}$$

where $\nabla_2^2 \equiv \partial^2/\partial x^2 + \partial^2/\partial y^2$ is the 2D Laplacian operator in the $[x, y]$ plane. Clearly, once B_z has resistively dissipated, i.e., for times much larger than the global resistive decay time τ, Φ is simply a solution of the 2D Laplace equation $\nabla_2^2\Phi = 0$.

Here comes the sneaky part. We take the curl of the induction equation. Upon substituting eq. (1.58), the z-component of the resulting expression yields

$$\nabla\times\nabla\times\left[\frac{\partial A}{\partial t} + \mathbf{u}_2\cdot\nabla A - \eta\nabla_2^2 A - \mathbf{u}_2\times\nabla\Phi\right] = 0, \tag{1.60}$$

with $\nabla\cdot(A\hat{\mathbf{e}}_z) = 0$ as a choice of gauge. Note that only one term involving Φ survives, because $\nabla\times\nabla\Phi = 0$ identically. In general, the above expression is only satisfied if the quantity in square brackets itself vanishes, i.e.,

$$\frac{\mathrm{D}A}{\mathrm{D}t} = \eta\nabla_2^2 A + \mathbf{u}_2\times\nabla\Phi, \tag{1.61}$$

This expression is identical to that obtained above for B_z, except for the presence of the source term $\mathbf{u}_2\times\nabla\Phi$. However, we just argued that for $t \gg \tau$, $\nabla_2^2\Phi = 0$. In addition, $\mathbf{B}$ vanishes on ∂V by assumption, so that the only possible asymptotic interior solutions are of the form Φ =const, which means that the source term vanishes in the limit $t \gg \tau$. From this point on eq. (1.61) is indeed identical to eq. (1.56), for which we demonstrated the inevitability of resistive decay, as per eq. (1.57). Therefore, dynamo action, i.e., maintenance of a magnetic field against resistive dissipation, is impossible in a planar flow for *any* 3D magnetic field.

Another powerful anti-dynamo theorem, in fact predating Zeldovich's, is due to T.G. Cowling. This anti-dynamo theorem is particularly important historically, since it rules out dynamo action for 3D but axisymmetric flows and magnetic fields, which happen to be the types of flows and fields one sees in the Sun, at least on the larger spatial scales. Many very mathematical proofs of Cowling's theorem can be found in the literature. Rather than trying to go over one of these, we will restrict ourselves here to a proof along the lines used in proving Zeldovich's theorem. Consider the most general forms for a steady axisymmetric flows and time-varying magnetic field in spherical coordinates[17]:

$$\mathbf{u}(r,\theta) = \nabla \times (\Psi(r,\theta)\hat{\mathbf{e}}_\phi) + \varpi\Omega(r,\theta)\hat{\mathbf{e}}_\phi \tag{1.62}$$

$$\mathbf{B}(r,\theta,t) = \nabla \times A(r,\theta,t)\hat{\mathbf{e}}_\phi + B(r,\theta,t)\hat{\mathbf{e}}_\phi \tag{1.63}$$

In analogy to the vector potential A, the stream function Ψ defines a *meridional flow*, i.e., a 2-D flow whose streamlines are fully contained in a meridian plane. For brevity of notation we will write

$$\mathbf{u}_p(r,\theta) = \nabla \times (\Psi(r,\theta)\hat{\mathbf{e}}_\phi), \tag{1.64}$$

with the understanding that $\mathbf{u}_p$ has no component in the ϕ-direction. Recall that under these circumstances the induction equation can be separated into the two components:

$$\frac{\partial}{\partial t}\left(\frac{B}{\varpi}\right) + \mathbf{u}_p \cdot \nabla\left(\frac{B}{\varpi}\right) = \frac{\eta}{\varpi}\left(\nabla^2 - \frac{1}{\varpi^2}\right)B - \left(\frac{B}{\varpi}\right)\nabla\cdot\mathbf{u}_p + [\nabla \times (A\hat{\mathbf{e}}_\phi)]\cdot\nabla\Omega, \tag{1.65}$$

$$\frac{\partial}{\partial t}(\varpi A) + \mathbf{u}_p \cdot \nabla(\varpi A) = \varpi\eta\left(\nabla^2 - \frac{1}{\varpi^2}\right)A, \tag{1.66}$$

and once again we assume that there are no sources of magnetic field exterior to the domain boundaries. The LHSs of eqs. (1.65)–(1.66) is again a

[17] Why do we not include a potential field component in eq. (1.63), as we did in the case of eq. (1.58)?

Lagrangian derivative for the quantities in parentheses, and the first term on each RHS is of course diffusion. The second term on the RHS of of eq. (1.65) vanishes for incompressible flow, and remains negligible for very subsonic compressible flow. The last term on the RHS, however, is a source term, in that it can lead to the growth of B *as long as* A *does not decay away.* However, there is no similar source-like term on the RHS of eq. (1.66), which governs the evolution of A.

This should now start to remind you of Zeldovich's theorem. In fact, eq. (1.66) is identical to eq. (1.56), for which we demonstrated the inevitability of resistive decay in the absence of sources exterior to the domain. This means that A will inexorably decay away, implying in turn that B will then also decay away once A has vanished. Since axisymmetric flows cannot maintain A against Ohmic dissipation, *there is no way for a 3D axisymmetric flow to act as a dynamo for a 3D axisymmetric magnetic field.* [18]. Cowling's theorem is not restricted to spherical geometry, and is readily generalized to any situation where both flow and field showing translational symmetry in one and the same spatial coordinate. Such physical systems are said to have an *ignorable coordinate.*

It is worth pausing and reflecting on what this means for the cellular flow considered earlier. This was a indeed a planar flow ($u_z = 0$), and moreover the magnetic field had an ignorable coordinate ($\partial \mathbf{B}/\partial z \equiv 0$)! This flow falls under the purview of both Zeldovich's and Cowling's theorems, so in retrospect our failure to find dynamo action is now understood.

When it was first demonstrated in 1934, Cowling's theorem had the effect of a very cold shower on geophysicists, planetary physicists and astrophysicists alike, all of whom were busily trying to explain the ubiquitous existence of magnetic fields in rotating cosmic bodies in terms of dynamo-like processes. Clearly, the way around Cowling's and Zeldovich's theorems is to consider flows and fields that are fully three-dimensional, and lack translational symmetry at least in the magnetic field.

Problems:

1. This problem lets you play a bit with the concept of magnetic energy (as defined in eq. (2.48).

[18]A fact often unappreciated is that Cowling's theorem does not rule out the dynamo generation of a *non-axisymmetric* 3D magnetic field by a 3D axisymmetric flow.

(a) Starting from the induction equation, obtain eq. (1.5).

(b) Show that in the absence of induction (meaning $\mathbf{U} = 0$), a force-free magnetic contained in a domain V will always decay.

(c) Show that your result in (b) remains true for magnetic fields that are not force-free, providing that the Poynting flux ($\propto \mathbf{E} \times \mathbf{B}$) vanishes at the domain boundary.

2. This problems gets you to redo the diffusive decay problem of §1.2 as a numerical 1-D eigenvalue problem. To avoid having to deal with the matching of your solutions to a potential field in $r/R > 1$, you can focus on the decay of purely toroidal magnetic fields If you choose the numerical avenue, then you may use the computing language of your choice, but please do include listings of all your codes with your solutions. Some useful Fortran-77 routines for the solution of tridiagonal systems of linear algebraic equations, together with instructions for use, can be obtained from the course Web Page:`http://www.hao.ucar.edu/public/education/astr7500.html`

   From the top of the main page, click on *Problems: Software and hints*,

   locate the appropriate subsection, and follow the instructions given there.

   (a) By assuming a θ-dependence in the form of the Associated Legendre Polynomials P_l^m, show that equation (2.16) reduces to eq. (2.17).

   (b) Use centered finite difference expressions (eqs. 2.[21]) to discretize the radial dependency, and solve the resulting system of algebraic equations using inverse iteration.

   (c) Obtain solutions for the first three angular degrees l and radial harmonics degrees n (for a total of 9 modes). Labels your solutions in terms of (l, n) values, and rank them according to decay time.

   (d) Compare the decay times of your toroidal eigenmodes to those of poloidal eigenmodes of corresponding angular and radial degrees, as shown on Fig. 2.1. Can you pick out a trend ? If so, try to come up with a qualitative explanation for it.

3. Recompute the cellular flow solution of §1.3 using periodic boundary conditions. Use second order centered finite differences to discretize the RHS of eq. (1.29), and the leapfrod scheme for time stepping. Make

use of the ghost cell formalism described in Box XX to enforce your periodic boundary conditions.

References to appropriate numerical boxes go here

(a) First compute a $\mathrm{R}_m = 10^3$ solution using the initial condition given by eq. (1.30) compute the time evolution of the total magnetic energy, and verify that it matches that plotted on Fig. **??**.

(b) Now repeat your calculation, but use this time as an initial condition a vector potential $A(y)$ that is gaussian in y and peaks at $y/L = 0.5$:

$$A(x,y,0) = 2B_0 \exp\left(-\frac{(y-L/2)^2}{(L/4)^2}\right).$$

Compare the resulting energy evolution to that you obtained earlier, and search your second solution for evidence of three more or less distinct amplification and decay phases:

(a) Growth of the field, on timescale $\sim L/u_0$;

(b) Enhanced resistive decay, on a timescale $\sim \mathrm{R}_m^{1/3} \equiv 10(L/u_0)$;

(c) A final, much slower decay phase, with timescale $\sim \mathrm{R}_m \equiv 10^3(L/u_0)$;

Bibliography:

The first detailed discussions of the diffusive decay of large-scale magnetic fields in astrophysical bodies are due to

Cowling, T.S. 1945, *Mon. Not. Roy. Astron. Soc.*, **105**, 166,
Wrubel, M.H. 1952, *Astrophys. J.*, **16**, 291.

On the numerical solution of algebraic eigenvalue problems in general, and on inverse iteration in particular, see

Golub, G.H., & Van Loan, C.F. 1989, *Matrix Computations (second edition)*, Baltimore: The Johns Hopkins University Press; §7.6.1 and 7.7.8.

Press, W.H., Teukolsky, S.A., Vetterling, W.T., & Flannery, B.P. 1992, *Numerical Recipes*, Second Ed., (Cambridge: Cambridge University Press), §11.7.

Chapter 11 of Press *et al.* also discusses numerical techniques that allow the computation of *all* eigenvalues of a matrix system, if you're interested in that. The book also contains a good introduction to the art of PDE discretization by finite differences. Among the numerous books discussing the calculation of macroscopic transport coefficients such as viscosity and electrical conductivity, starting from a microscopic point of view, our preference goes to an old classic:

Spitzer, L. Jr. 1962, *Physics of Fully Ionized Gases* (second ed.), New York: Wiley Interscience.

On the inference of large-scale magnetic fields on slowly rotating chemically peculiar stars, see

Deutsch, A.J. 1970, *Astrophys. J.*, **159**, 985,
Borra, E.F., Lanstreet, J.D., & Mestel, J. 1982, ARA&A, 20, 191,

and references therein. Magnetic flux expulsion from regions of closed streamlines is discussed in many textbooks dealing with magnetohydrodynamics. Analytical solutions for some specific cellular flows can be found for example in

Moffatt, H.K. 1978, *Magnetic field generation in electrically conducting fluids* (Cambridge: Cambridge University Press),
Parker, E.N. 1979, *Cosmical Magnetic Fields*, Oxford: Clarendon Press, chap. 16.

but for the first and last word on this topic, you should consult

Weiss, N.O. 1966, Proc. Roy. Soc. London A, 293, 310,
Rhines, P.B., & Young, W.R. 1983, J. Fluid Mech., 133, 133.

The Rhines & Young paper contains clean analytical examples of the two successive dissipative phases with characteristic timescales proportional to $\mathrm{R}_m^{1/3}$ and R_m, as discussed in §2.3.2. Flux expulsion is of course not restricted to 2-D flow; for a nice example in 3-D see

Galloway, D.J., & Proctor, M.R.E. 1983, *Geophys. Astrophys. Fluid Dyn.*, **24**, 109.

On the possible symmetrization of the Saturnian magnetic field by deep-seated differential rotation, see

Stevenson, D.J. 1982, *Geophys. Astrophys. Fluid Dyn.*, **21**, 113-127
Kirk, R.L., & Stevenson, D.J. 1987, *Astrophys. J.*, **316**, 836-846

An insightful discussion of the symmetrization process in more general terms is that of

Rädler, K.-H. 1986, On the effect of differential rotation on axisymmetric and non-axisymmetric magnetic fields in cosmic bodies, in *Proceedings of the Joint Varenna-Abastumani International School and Workshop*, ESA Spec. Pub. SP-251, 569-574

The Saturnian calculations alluded to at the close of §2.3.5 are by Charbonneau & Bagenal (unpublished manuscript); ask me about it if you are interested. As for planetary magnetic field observations, a good recent overview is

Connerney, J.E.P. 1993, *J. Geophys. Res.*, **98**, 18659-18679

On anti-dynamo theorems, see

Cowling, T.G. 1933, *Mon. Not. Roy. Astron. Soc.*, **94**, 39,
Bullard, E.C., & Gellman, H., *Phil. Trans. R. Soc. London A*, **247**, 213,
Zeldovich, Ya. B. 1956, J. Exp. and Theoretical Physics, 31, 154 [Russian]; XX, YYY [English],
Zeldovich, Ya. B., & Ruzmaikin, A.A. 1980, J. Exp. and Theoretical Physics, 78, 980 [Russian]; XX, YYY [English],

as well as pages XXX-ff and 538–ff, respectively, of the books by Moffatt and Parker listed above. English translations of the last two papers are also reprinted in *Selected Works of Yakov Borisovich Zeldovich*, vol. 1 (ed. J.P. Ostriker, Princeton, 1992).

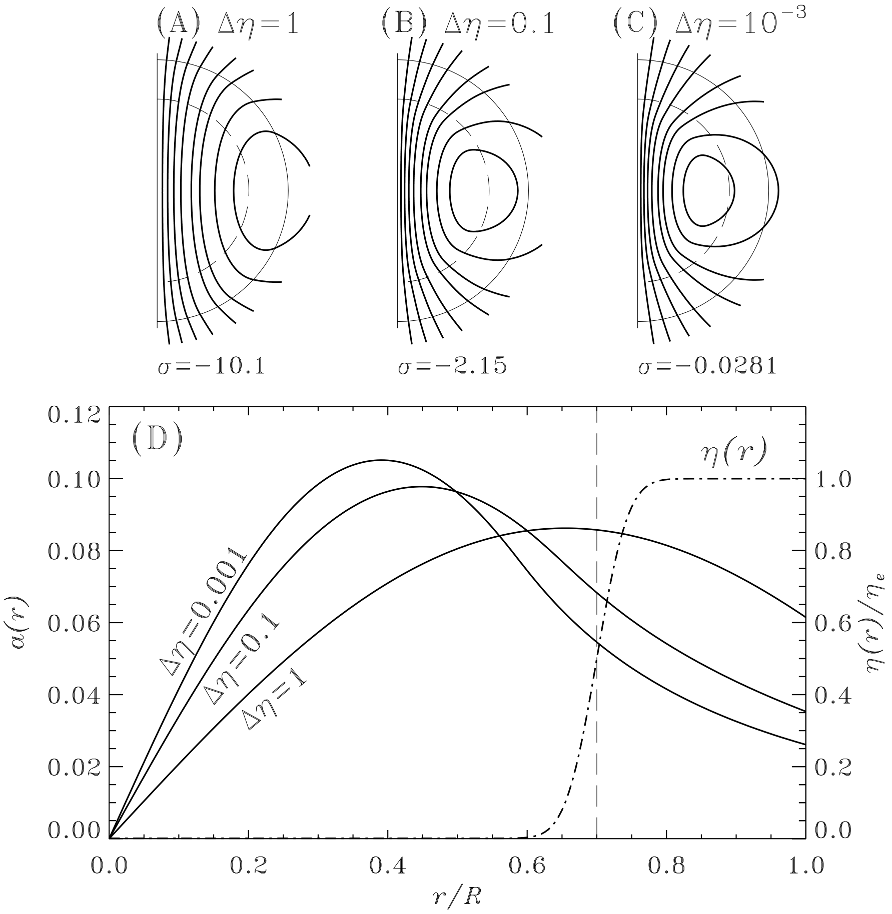

Figure 1.1: Panels (A) through (C): The slowest decaying ($\ell = 1$) poloidal eigenmodes in a solar model embedded in a vacuum, with the diffusivity computed using eq. (1.19) with $r_c/R = 0.7$ and $w/R = 0.05$, for decreasing values of the core-to-envelope diffusivity ratio ($\Delta\eta$). Panel (D) shows the corresponding radial eigenfunctions, together with the diffusivity profile for $\Delta\eta = 10^{-3}$ (dash-dotted line). The dashed line indicates the core-envelope interface

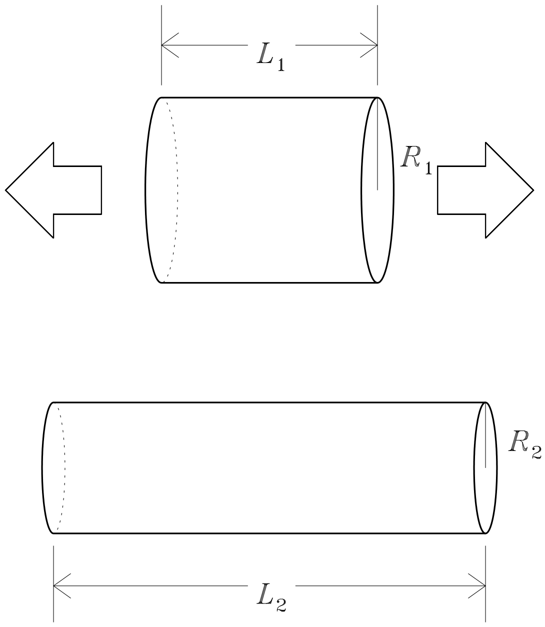

Figure 1.2: Stretching of a magnetized cylindrical fluid element flow tube by a diverging flow. The magnetic field is horizontal within the tube, has a strength B_1 originally, and B_2 after stretching. In the flux-freezing limit mass conservation within the tube requires its radius to decrease, which in turn leads to field amplification (see text).

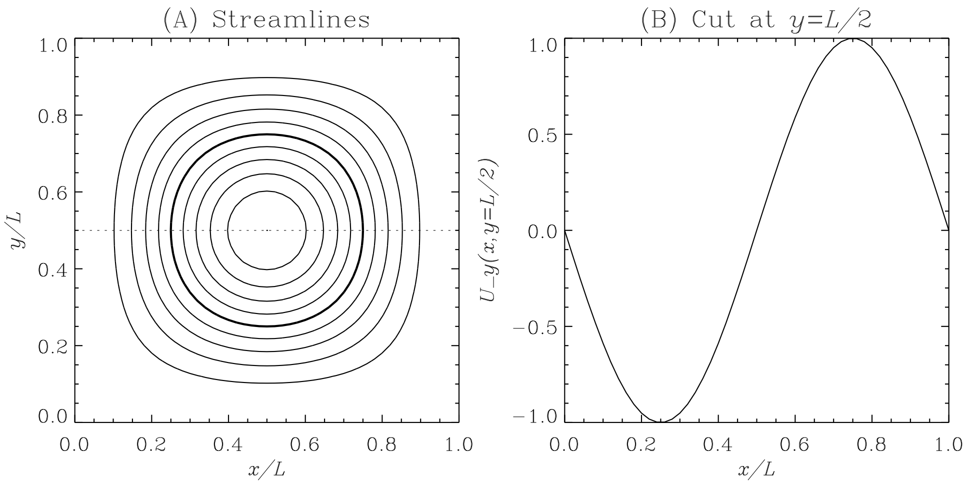

Figure 1.3: Counterclockwise cellular flow generated by the streamfunction given by eq. (1.28). Part (A) shows streamlines of the flow, with the thicker streamline corresponding to $\Psi = u_0 L/(2\pi)$, on which the flow attains its maximum speed u_0. Part (B) shows the profile of $U_y(x)$ along an horizontal cut at $y = 1/2$. A "typical" length scale for the flow is then $\sim L$.

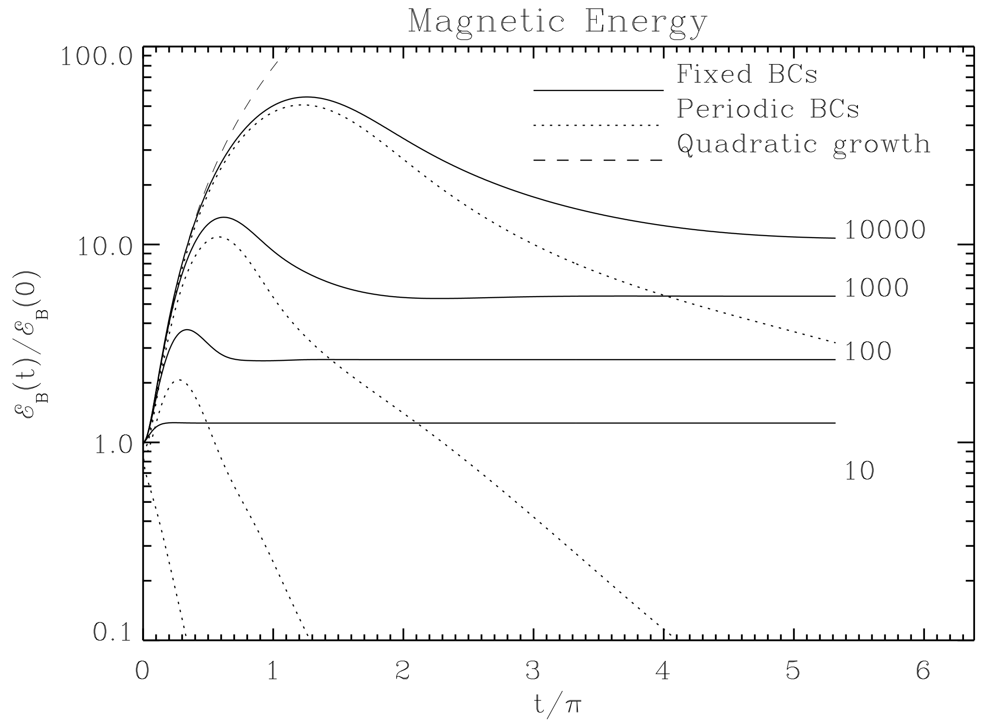

Figure 1.4: Evolution of the magnetic energy for solutions with increasing R_m. The solutions have been computed over 10 turnover times, at which point they are getting reasonably close to steady-state, at least as far as magnetic energy is concerned. One turnover time corresponds to $t/\pi = 0.532$.

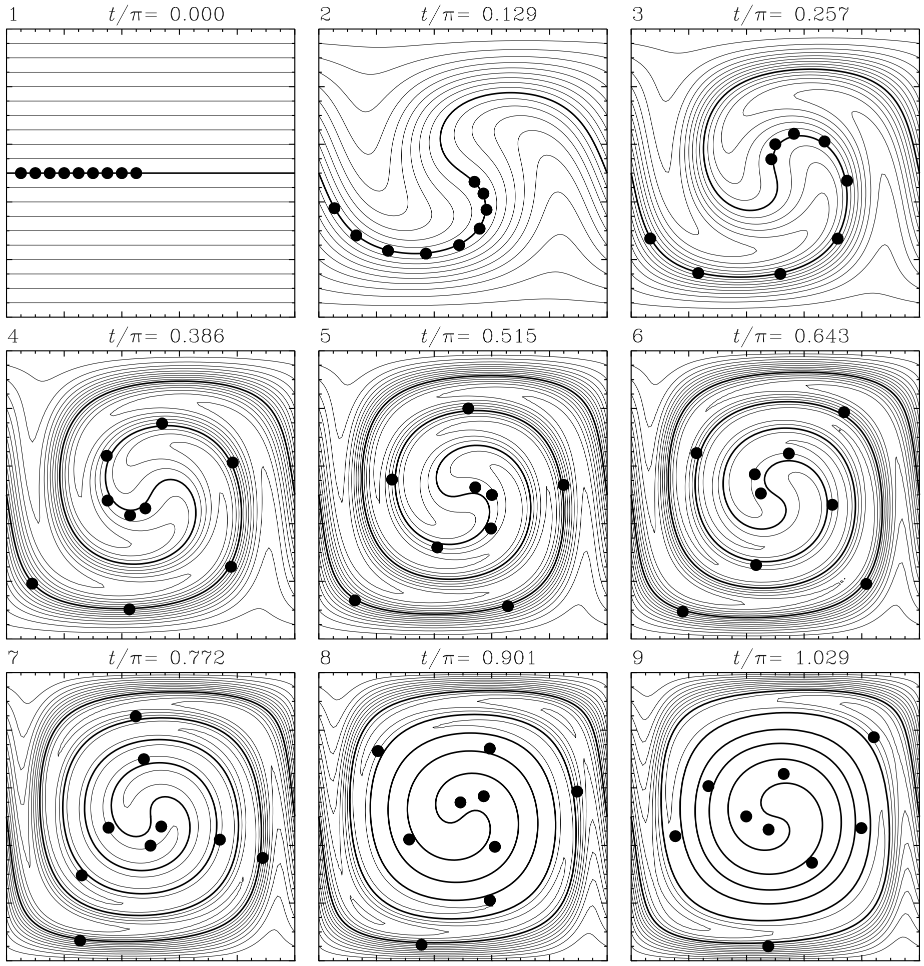

Figure 1.5: Solution to equation (1.29) starting from an initially horizontal magnetic field. The panels show the shape of the magnetic fieldlines at successive times. The x- and y-axes are horizontal and vertical, respectively, and span the same range as on Fig. (1.3.2A), namely $x, y \in [0, L]$. Time t is in units of L/u_0. The solid dots are "floaters", i.e., Lagrangian marker passively advected by the flow.

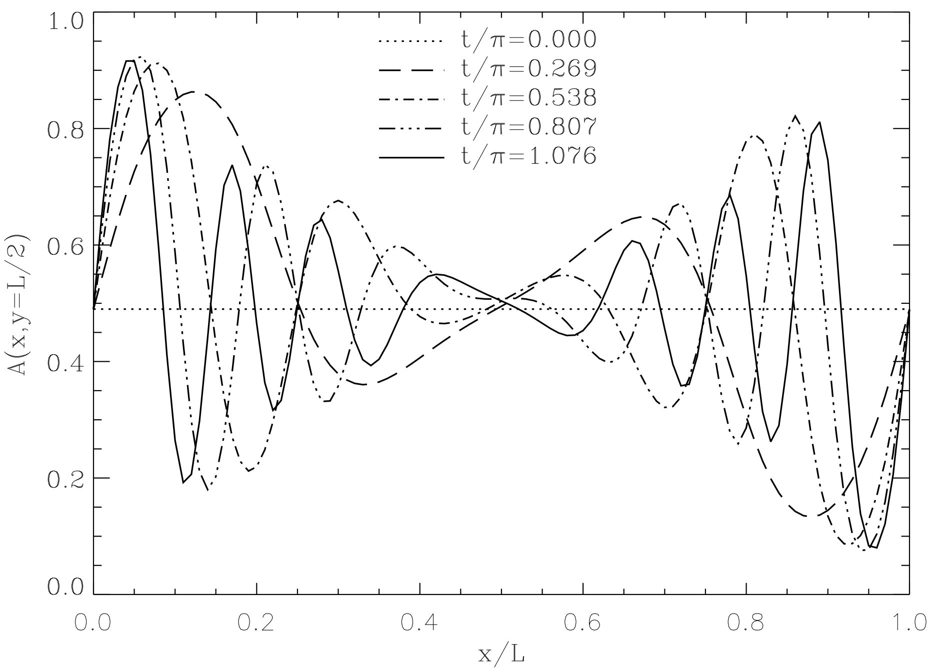

Figure 1.6: Cuts of a $\mathrm{R}_m = 10^4$ solution along the coordinate line $y = 0.5$, at successive times. The dashed and dash-dotted lines corresponds, respectively, to the fifth and ninth frames on Figures 1.3.2 and 1.3.2. Note how the "typical" length scale ℓ for the solution decreases with time, from $\ell/L \sim 0.25$ at $t/\pi = 0.269$, down to $\ell/L \sim 0.05$ after two turnover times ($t/\pi = 1.065$).

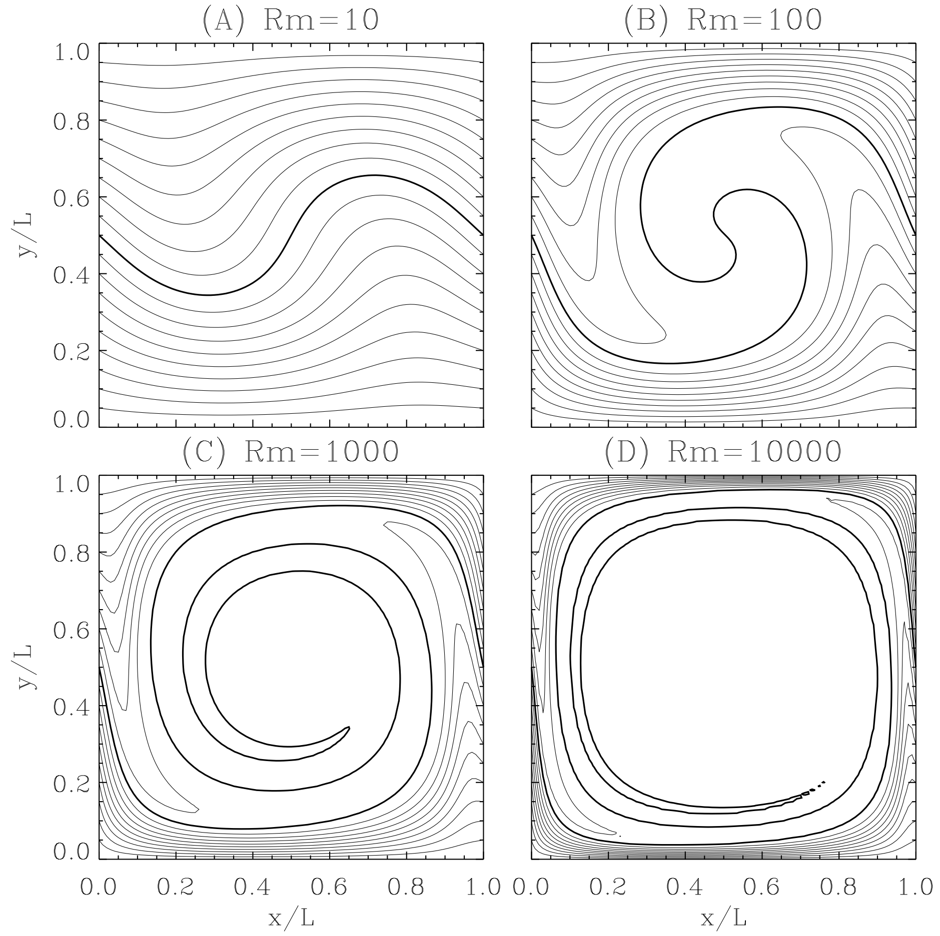

Figure 1.7: Steady-state solutions to the cellular flow problem, for increasing values of the magnetic Reynolds number R_m. The $R_m = 10^4$ solution is at the resolution limit of the $N_x \times N_y = 100 \times 100$ mesh used to obtain these solutions, as evidenced on part (D) by the presence of small scale irregularities where magnetic fieldlines are sharply bent. Note how, in the higher R_m solutions, magnetic flux is expelled from the center of the flow cell. With $\mathcal{E}_B(0)$ denoting the energy of a purely horizontal field with same normal boundary flux distribution (see panel 1 of Fig. 1.3.2), the magnetic energy for these steady states is $\mathcal{E}_B/\mathcal{E}_B(0) = 1.37$, 2.80, 5.81 and 11.75, respectively, for panels (A) through (D).

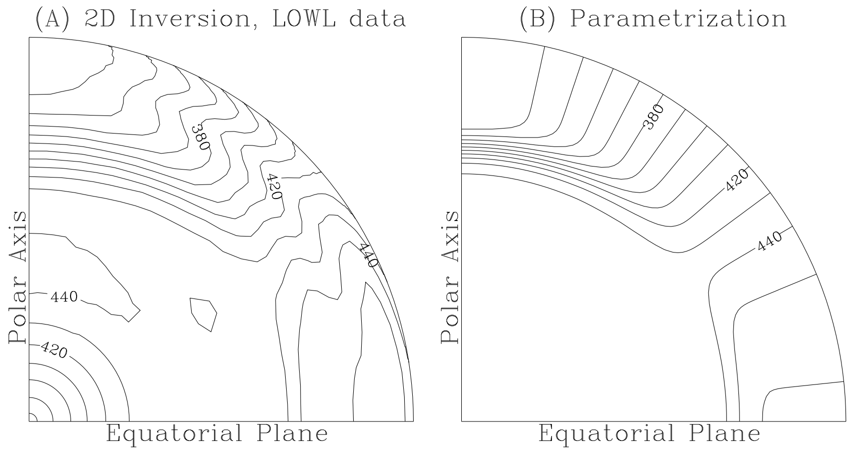

Figure 1.8: [F2.12] Regularized least-square inversion for the internal solar angular velocity, obtained with the LOWL 2-year frequency splitting dataset (left), and parametric representation obtained from eq. (1.49) (right). The angular velocity is shown in a meridional quadrant, in the form of of angular *frequency*, in the range $340 \leq \Omega/2\pi \leq 460\,$nHz with 10 nHz spacing.

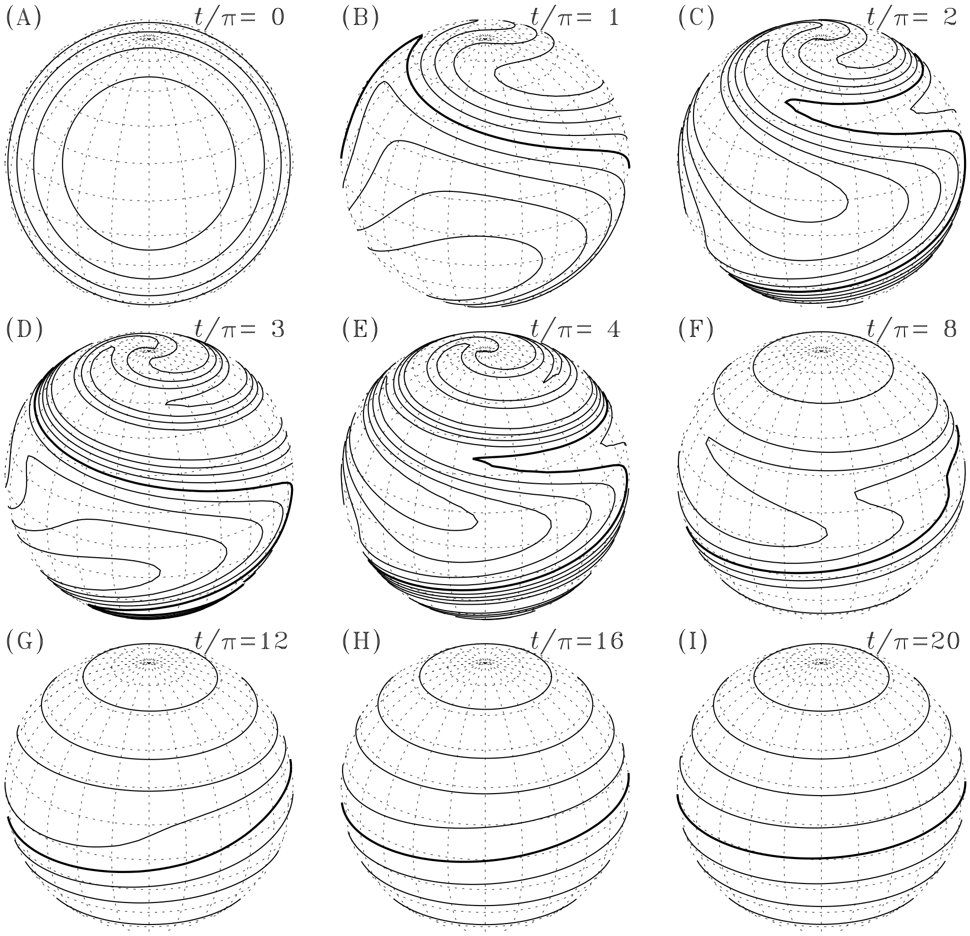

Figure 1.9: Symmetrization of an inclined dipole in a electrically conducting sphere in a state of solar-like axisymmetric differential rotation. Each panel shows contours of constant B_r at the surface of the sphere. The solution is matched to a potential in the exterior ($r/R > 1$). The differential rotation is given by eq. (1.49). Time is given in units of the turnover time, defined via eq. (1.51.